Published in final edited form as:

Cell Calcium. 2007 January ; 41(1): 51–61. doi:10.1016/j.ceca.2006.04.032.

TRPM4 controls insulin secretion in pancreatic β-cells

Henrique Cheng[a,1,2], **Andreas Beck**[a,1], **Pierre Launay**[b,3], **Stefan A. Gross**[a], **Alexander J. Stokes**[a], **Jean-Pierre Kinet**[b], **Andrea Fleig**[a], and **Reinhold Penner**[a,*]

[a]Laboratory of Cell and Molecular Signaling, Center for Biomedical Research at The Queen's Medical Center and John A. Burns School of Medicine at the University of Hawaii, 1301 Punchbowl St., UHT 8, Honolulu, HI 96813, United States

[b]Department of Pathology, Beth Israel Deaconess Medical Center and Harvard Medical School, Boston, MA 02215, United States

Abstract

TRPM4 is a calcium-activated non-selective cation channel that is widely expressed and proposed to be involved in cell depolarization. In excitable cells, TRPM4 may regulate calcium influx by causing the depolarization that drives the activation of voltage-dependent calcium channels. We here report that insulin-secreting cells of the rat pancreatic β-cell line INS-1 natively express TRPM4 proteins and generate large depolarizing membrane currents in response to increased intracellular calcium. These currents exhibit the characteristics of TRPM4 and can be suppressed by expressing a dominant negative TRPM4 construct, resulting in significantly decreased insulin secretion in response to a glucose stimulus. Reduced insulin secretion was also observed with arginine vasopressin stimulation, a Gq-coupled receptor agonist in β-cells. Moreover, the recruitment of TRPM4 currents was biphasic in both INS-1 cells as well as HEK-293 cells overexpressing TRPM4. The first phase is due to activation of TRPM4 channels localized within the plasma membrane followed by a slower secondary phase, which is caused by the recruitment of TRPM4-containing vesicles to the plasma membrane during exocytosis. The secondary phase can be observed during perfusion of cells with increasing $[Ca^{2+}]_i$, replicated with agonist stimulation, and coincides with an increase in cell capacitance, loss of FM1-43 dye, and vesicle fusion. Our data suggest that TRPM4 may play a key role in the control of membrane potential and electrical activity of electrically excitable secretory cells and the dynamic translocation of TRPM4 from a vesicular pool to the plasma membrane via Ca^{2+}-dependent exocytosis may represent a key short- and midterm regulatory mechanism by which cells regulate electrical activity.

Keywords

TRPM4; Dominant-negative TRPM4; Exocytosis; Insulin; Pancreatic β-cell

*Corresponding author. Tel.: +1 808 585 5366; fax: +1 808 585 5377. rpenner@hawaii.edu (R. Penner).

[1]These authors contributed equally to this work.

[2]Present address: Department of Comparative Biomedical Sciences, School of Veterinary Medicine, Louisiana State University, Baton Rouge, LA 70803, United States.

[3]Present address: INSERM U699, Avenir Group, Bichat Medical School, 75018 Paris, France.

1. Introduction

The transient receptor potential (TRP) proteins are a family of ion channels which are divided into three major subfamilies: the TRPC “Canonical”, the TRPV “Vanilloid”, and the TRPM “Melastatin” [1–3]. The TRPM subfamily consists of eight members and information regarding their physiological function has just begun to surface. TRPM4 is a widely expressed calcium-activated non-selective cation (CAN) channel that conducts mainly Na^+ and K^+ without appreciable permeation to Ca^{2+}. It has a single channel conductance of ~25 pS and is directly activated by $[Ca^{2+}]_i$. Two splice variants have been described, a short TRPM4a, which lacks 174 amino acid residues at the N-terminus [4], and the long form TRPM4b [5], which we will refer to as TRPM4 throughout this manuscript. In non-excitable cells such as T-lymphocytes, the TRPM4-mediated depolarization reduces the driving force for Ca^{2+} entry through Ca^{2+} release-activated Ca^{2+} channels (CRAC) with significant impact on Ca^{2+} oscillations and cytokine production [6]. TRPM4 is also implicated in myogenic constriction and cardiac function [7,8], suggesting that it may critically regulate Ca^{2+} entry mechanisms in electrically excitable cells as well.

Changes in membrane potential during glucose stimulation are crucial for determining the shape and frequency of Ca^{2+} oscillations in β-cells, because each depolarization induces a concomitant rise in the $[Ca^{2+}]_i$ that triggers insulin secretion [9,10]. Impaired Ca^{2+} oscillations result in deficiencies in insulin secretion in certain forms of type 2 diabetes in humans and rodents [11–13]. The cellular and molecular components involved in membrane depolarization of β-cells have not been fully identified. Glucose stimulates insulin secretion by activating two pathways [11]: the triggering pathway involves a sequence of events beginning with glucose uptake, its metabolism and increase in ATP–ADP ratio, followed by closure of ATP-sensitive K^+ (K_{ATP}) channels. Closure of K_{ATP} channels triggers membrane depolarization with opening of voltage-dependent calcium channels (VDCCs) and Ca^{2+} influx [14], however, this requires the additional presence of a depolarizing current that so far has not been identified. The opening of VDCCs is dependent on the cell membrane potential, which is around −70 mV at rest. Depolarization activates VDCCs, with peak Ca^{2+} currents around 0 mV [15–18]. TRPM4 currents reverse around 0 mV, and enhanced channel activity depolarizes cells from negative resting membrane potentials [5]. In this scenario, TRPM4 is an ideal candidate for controlling VDCC activation. Therefore, we hypothesized that TRPM4 is a key regulatory component that controls membrane potential and provides the basis for Ca^{2+} entry through VDCCs. The amplifying pathway, also referred to as the K_{ATP} independent pathway, depends on an already elevated $[Ca^{2+}]_i$. It acts by increasing the efficiency of Ca2+ on secretion.

In this study, we investigated the functional role of TRPM4 during glucose-induced insulin secretion in β-cells using the rat insulinoma cell line INS-1 as a model system. We find that TRPM4 is not only abundantly expressed in these cells, but critically regulates insulin secretion. Suppression of TRPM4 by a dominant negative construct of TRPM4 suppressed the normal pulsatile pattern of insulin secretion. Our results also indicate that translocation of TRPM4-containing vesicles via Ca^{2+}-dependent exocytosis may represent a mechanism by which β-cells regulate the pool of TRPM4 channels in the plasma membrane.

2. Methods

2.1. Electrophysiology

2.1.1. Solutions—HEK-293 cells grown on glass coverslips were transferred to the recording chamber and kept in a standard modified Ringer's solution of the following composition (in mM): NaCl 140, KCl 2.8, $CaCl_2$ 1, $MgCl_2$ 2, glucose 10, HEPES-NaOH 10, pH 7.2, with osmolarity adjusted to around 300 mOsm. For experiments with INS-1 cells, the external solution was further supplemented with 300 nM TTX, 100 μM 4,4′-diisothiocyano-2,2′-stilbene disulphonic acid (DIDS) and 10 mM tetraethylammonium (TEA). Intracellular pipette-filling solutions for HEK-293 cells contained (in mM): K-glutamate 140, NaCl 8, $MgCl_2$ 1, K-BAPTA 10, HEPES-KOH, pH 7.2 adjusted with KOH. The internal solution for INS-1 cells contained (in mM): Cs-glutamate 140, NaCl 8, $MgCl_2$ 1, Cs-BAPTA 10, HEPES-CsOH, pH 7.2 adjusted with CsOH. In experiments where $[Ca^{2+}]_i$ was buffered to elevated levels, $CaCl_2$ was added as necessary (calculated with WebMaxC http://www.stanford.edu/~cpatton/webmaxcS.htm). Solution changes were performed by bath perfusion for calcium imaging experiments.

2.1.2. Patch-clamp—Patch-clamp experiments were performed in the tight-seal whole-cell configuration at 21–25 °C. High-resolution current recordings were acquired by a computer-based patch-clamp amplifier system (EPC-9, HEKA, Lambrecht, Germany). Patch pipettes had resistances between 3 and 6 MΩ after filling with the standard intracellular solution. Immediately following establishment of the whole-cell configuration, voltage ramps of 50 ms duration spanning the voltage range of −100 to +100 mV were delivered from a holding potential of 0 mV at a rate of 0.5 Hz over a period of 600–1000 s. All voltages were corrected for a liquid junction potential of 10 mV between external and internal solutions when using glutamate as intracellular anion. Currents were filtered at 2.9 kHz and digitized at 100 μs intervals. Capacitive currents and series resistance were determined and corrected before each voltage ramp using the automatic capacitance compensation of the EPC-9. The low-resolution temporal development of membrane currents was assessed by extracting the current amplitude at −80 mV or +80 mV from individual ramp current records. Data analysis, statistical analysis and graphical display of patch-clamp experiments were done using the Igor Pro 5 software program (Wavemetrics).

2.2. RT-PCR and immunoprecipitation

Total RNA was extracted with RNAzol according to the manufacturer's protocol (ISO-TEX Diagnostics, Friendswood, TX). DNAse I-treated RNA was used for reverse transcription using RETROscript Kit (Ambion, Austin, TX). PCR was performed by a standard method using Advantage Polymerase PCR Kit (Clonetch, Palo Alto, CA). For immunoprecipitation, cells were lysed for 30 min at 4 °C in Tris buffer pH 7.5 containing 1% Triton X-100 (Bio-Rad, Hercules, CA) and protease inhibitors. Immunoprecipitation was resolved by 6% SDS-PAGE blotted with the rabbit polyclonal antisera against the C-terminal region of human TRPM4 and visualized by Enhanced Chemiluminescence (Amersham Pharmacia Biotech).

2.3. Measurement of insulin secretion

Truncated forms of TRPM4 cDNA were cloned into a modified version of the pCDNA4/TO vector with an N-terminal V5 epitope tag. The correct sequence of V5-ΔN-TRPM4 expression construct was confirmed by DNA sequencing. Constructs were transfected in INS-1 cells using Lipofectamine 2000™ and Plus Reagent (Invitrogen, Carlsbad, CA) 24 h after cells were plated and experiments were done 48–72 h post transfection. Control cells were transfected with reagents without the ΔN-TRPM4 DNA. INS-1 cells between p47 and p55 were used in these experiments.

2.3.1. Static incubation experiments—INS-1 cells were plated into 24-well plates at ~5×10^5 cells/well and grown for 3–4 days. Measurement of insulin secretion was accomplished by replacing the culture medium with modified KRB containing (in mM): NaCl 136, KCl 4.8, $CaCl_2$ 2.5, KH_2PO_4 1.2, $MgSO_4$ 1.2, $NaHCO_3$ 5, HEPES 10, glucose 4 and 0.1% BSA, pH 7.4. After a 15-min equilibration period at 37 °C, cells were exposed to different treatments and allowed to incubate for 15 min. At the end of each experiment, the KRB was collected for insulin RIA [19] and the number of cells quantified. Each treatment was done in quadruplicates and repeated three times.

2.3.2. Perifusion experiments—The perifusion system used was as previously described [19]. INS-1 cells were grown on 22 mm round glass coverslips inside a multi-well culture plate for 3–4 days until confluency (~10^6 cells). Each coverslip was then removed from each well and mounted inside a 25 mm perifusion chamber (Millipore Swinnex Filter Holders, Waters, Milford, MA, U.S.A.) with cells facing inside the chamber. Initially, the cells were perifused for a 20 min equilibration period at 37 °C with modified KRB. The flow rate was adjusted to 0.5 ml/min prior to experiments and samples collected at 30 s intervals. At the end, the glass coverslips were removed from the chambers and the number of cells quantified. Insulin concentration from effluent samples were measured by RIA. Experiments were replicated three times with different cell passages.

2.4. Confocal microscopy

Exponentially growing Flag-TRPM4-transfected HEK-293 cells were plated on 12 mm glass coverslips and incubated overnight. After 24 h cells were incubated with 1 μM Cell Tracker Green (Molecular Probe, Eugene, OR) during 30 min at 37 °C. Cells were then activated with 1 μM ionomycin to induce exocytosis. The activation reaction was stopped and cells fixed by incubating coverslips in 100% methanol 10 min at −20 °C. All subsequent steps were carried out at room temperature. Cells were rinsed in PBS and incubated in blocking solution (PBS–0.5% FSG) for 45 min to reduce nonspecific binding of antibodies. After rinsing coverslips three times in PBS–0.02% FGS, primary and secondary antibodies were added sequentially for 30 min. The Flag antibody was used at 1/5000 and secondary antibody GAM-Alexa-568 at 1/6500. Coverslips were then inverted into 10 ml of mounting medium containing antifade agents (Biomeda Corp., Foster City, CA). Confocal images were obtained using a Bio-Rad MRC 1024ES laser-scanning microscope (Bio-Rad, Hercules, CA).

2.5. Fluorescence imaging and analysis

Exocytosis was monitored using a membrane marker FM1-43. Cells were loaded with 10 μM FM1-43 for 24 h in culture medium and prior to experiments were washed and equilibrated for 15 min in standard buffer solution. Fluorescence of FM1-43 was excited with 480 nm and collected at 535 nm. Data acquisition from Ca^{2+} measurement experiments were obtained with a dual excitation fluorometric imaging system (TILL-Photonics, Gräfelfingen, Germany) and controlled by TILLvisION software. Fura-2 AM loaded cells (5 μM/30 min/37 °C) were excited by wavelengths of 340 and 380 nm. Fluorescence emissions of several cells were sampled at 1 Hz and computed into relative ratio units of the fluorescence intensity of the different wavelengths. Data analysis, statistical analysis and graphical display of imaging data were done using the Igor Pro 5 software program (Wavemetrics).

2.6. Data analysis

Results from insulin secretion experiments were analyzed using SAS PROC MIXED procedure and a randomized block design. Individual mean comparisons were performed using *F*-test. The significance level was set at $P < 0.05$.

3. Results

We first probed for TRPM4 in β-cells and investigated whether currents with the characteristics of the channel could be detected. In addition to MIN-6 cells [20], we detected TRPM4 transcripts in HIT-T15 (hamster derived), INS-1 and RINm5F (rat derived) cells. The cDNA of Jurkat T-cells were used as positive control [6] (Fig. 1A). To confirm protein expression in the plasma membrane, we used a rabbit polyclonal anti-peptide antibody against TRPM4. The channel was detected in INS-1 and RINm5F cell lines and Jurkat T-cells as a single band with the predicted molecular size (Fig. 1B). No protein was detected after immunoprecipitation with an irrelevant control antibody (C). Next, we selected INS-1 cells for the functional characterization, because they represent a widely accepted model for β-cell metabolism and insulin biosynthesis [21–23]. Perfusion of cells with 0.5–3 μM $[Ca^{2+}]_i$ induced TRPM4 currents in a concentration-dependent manner (Fig. 1C) that typically exhibited a biphasic pattern. The first phase was observed within seconds after establishment of whole-cell configuration (Fig. 1C upper panel) and was followed by a secondary phase that gradually developed during the course of experiments (Fig. 1C lower panel). The current–voltage relationships taken from representative cells at the peak of the first phase and at 600 s for the second phase resemble those of TRPM4 (Fig. 1F and G). A dose–response fit to the first phase and secondary phase gave EC_{50} values of 1.7 μM and 1.2 μM, respectively (Fig. 1D). Interestingly, the appearance of the secondary phase correlated with an increase in cell capacitance (Fig. 1E). We repeated the above data set in the HIT-T15 β-cell model, as TRPM4 could be detected there by immunoprecipitation as well using the rabbit polyclonal anti-peptide antibody against TRPM4 (data not shown). In these cells we also observed a first phase and a secondary phase developing in parallel to an increase in cell size and comparable dose–response curves (data not shown).

Because multimerization of TRPM4 is likely required to form the proper pore structure of the channel, we utilized a truncated form lacking the first 177 amino acids in the N-terminus to obtain a dominant negative effect (ΔN-TRPM4) and investigated its role on insulin secretion. Previously, we have shown the ability to this mutant form to associate with endogenous TRPM4 channels and suppress their activity [6]. Exposure of control, mock-transfected INS-1 cells to 4, 10 and 25 mM glucose stimulated insulin secretion in a concentration-dependent manner, where glucose at 25 mM resulted in a ~2.2-fold increase in secretion compared to basal 4 mM. Suppression of endogenous TRPM4 by the ΔN-TRPM4 construct significantly decreased the response to 10 and 25 mM glucose ($P < 0.05$) compared to control cells (Fig. 2A) and glucose at 25 mM resulted in a much reduced ~1.3-fold increase in secretion compared to basal 4 mM in ΔN-TRPM4 cells. Likewise, the response to 1 μM arginine vasopressin (AVP) was significantly decreased ($P < 0.05$) in ΔN-TRPM4 compared to control cells (Fig. 2B). However, insulin secretion in response to 20 mM KCl or 1 mM L-arginine, which both depolarize cells directly and independently of TRPM4, did not differ.

In β-cells, oscillations in the membrane potential result in oscillations in Ca^{2+} signals, because each depolarization opens VDCCs and Ca^{2+} influx occurs. As a result, insulin is secreted in a pulsatile fashion. To investigate the impact of TRPM4 on the pulsatile secretion pattern, we utilized a perifusion system to measure secretion in response to a glucose stimulus in ΔN-TRPM4 cells. TRPM4 suppression significantly decreased insulin secretion to 25 mM glucose compared to control, mock-transfected INS-1 cells (Fig. 2C). The typical oscillations observed with glucose stimulation were absent in ΔN-TRPM4 cells. At the end of experiments, cells were depolarized with 20 mM KCl to test their viability and this response remained unaffected.

Electrophysiological recordings of TRPM4 currents in β-cells showed a biphasic pattern during perfusion with elevated $[Ca^{2+}]_i$. The first phase activated within seconds after establishment of whole-cell configuration [5]. We hypothesized that based on its rapid kinetics, the first phase might be due to activation of TRPM4 channels already present in the plasma membrane and that the secondary phase might result from translocation and incorporation of TRPM4-containing vesicles to the plasma membrane during exocytosis. The latter notion is based on the observation that an increase in cell capacitance correlated with the development of the secondary phase. To characterize this secondary phase, we utilized HEK-293 cells overexpressing TRPM4 to facilitate the visualization of currents/capacitance changes under different $[Ca^{2+}]_i$ concentrations. In agreement with the observations in β-cells, perfusion with 0.1–10 μM $[Ca^{2+}]_i$ induced biphasic currents in a concentration-dependent manner (Fig. 3A and B). The first phase was observed within seconds after establishment of the whole-cell configuration followed by a secondary phase that gradually developed during the course of experiments. The current–voltage relationships taken from representative cells at the peak of the first and secondary phases for different Ca^{2+} concentrations are typical of TRPM4 (Fig. 3E and F). A dose–response fit to the first phase and secondary phase gave EC_{50} values of 1.2 and 1.3 μM, respectively (Fig. 3C). As in the β-cells, the appearance of the secondary phase also correlated with an increase in cell capacitance (Fig. 3D).

To test whether the secondary phase was indeed due to exocytosis, we labeled intracellular vesicles with the styryl dye FM1-43, which is used as fluorescent probe for membrane trafficking [24,25]. Perfusion of cells with 1 μM Ca^{2+} resulted in greater fluorescence loss compared to 100 nM or intact control cells (Fig. 4A and B; average fluorescence changes in Fig. 4C). Further, we obtained electrophysiological recordings from cells loaded with FM1-43 dye to determine if there was an increase in capacitance during fluorescence loss. Perfusion with 1 μM $[Ca^{2+}]_i$ increased membrane capacitance (Fig. 4D) that correlated with fluorescence loss (see Fig. 4C) during the development of the secondary phase (see Fig. 4E). This was not observed in cells perfused with 100 nM $[Ca^{2+}]_i$. These findings suggest that vesicles containing TRPM4 channels are recruited to the plasma membrane, since fluorescence loss and increased capacitance and the appearance of the secondary phase all correlated temporally.

To visualize TRPM4 translocation, HEK-293 cells bearing a Flag-tagged version of TRPM4 were loaded with cytotracker green dye before stimulation with 1 μM ionomycin. Under confocal microscopy, the projected stacks showed a membrane translocation of TRPM4 (in red) after exocytosis (Fig. 5A). The translocation and incorporation of TRPM4 to the plasma membrane led us to test whether the channel itself was involved in the exocytotic process. We reasoned that if TRPM4 plays a role in the exocytotic process, the ΔN-TRPM4 construct should not only inhibit currents carried by TRPM4 but might also affect capacitance changes. HEK-293 cells expressing ΔN-TRPM4 constructs indeed had significantly smaller TRPM4 current amplitudes compared to controls when perfused with 1 μM Ca^{2+} (Fig. 5B), however, there was no obvious effect on exocytosis as indicated by capacitance measurements (Fig. 5C).

Since TRPM4 significantly reduced insulin secretion in response to glucose and AVP stimulation, we examined whether the secondary phase of current recruitment could be observed with agonist stimulation. We hypothesized that if an initial carbachol treatment increased $[Ca^{2+}]_i$ leading to exocytosis and recruitment of TRPM4 vesicles, a second application would result in greater currents due to an increased number of channels in the plasma membrane. Utilizing Ca^{2+} imaging techniques, fura-2-AM loaded cells were stimulated with 1 mM carbachol for 200 s followed by washout and a second stimulation (Fig. 6A). The first carbachol application induced a sharp peak in $[Ca^{2+}]_i$ that was followed by a sustained secondary phase due to Ca^{2+} influx necessary for exocytosis and TRPM4 currents were less than 1 nA in amplitude. After a washout period, a second carbachol application resulted in a smaller Ca^{2+} signal, however now the currents carried by TRPM4 were around 10 nA in amplitude. Control cells that received single carbachol stimulation produced a small increase in TRPM4 current following the first agonist application, but failed to develop the secondary phase (Fig. 6B). The current–voltage relationships from a representative cell before and after carbachol stimulation for both time periods resemble those of TRPM4 (Fig. 6C). In these experiments, exocytosis was confirmed by an increase in cell capacitance after carbachol stimulation (Fig. 6D).

4. Discussion

The present study was undertaken to investigate the functional role of TRPM4 in pancreatic β-cells and to provide insights on the mechanism by which these cells regulate the pool of TRPM4 in the plasma membrane. We have found that TRPM4 is not only expressed in a variety of β-cell lines, but critically regulates insulin secretion during glucose stimulation. Suppression of TRPM4 by a dominant negative effect significantly decreased secretion with profound impact on the amplitude of insulin oscillations. Pulsatile insulin release is caused by oscillations in $[Ca^{2+}]_i$, driven by the opening and closure of VDCCs, which in turn is dependent on the cell's membrane potential. At rest, this potential is controlled mainly by a hyperpolarizing current carried by K_{ATP} channels [26]. As ATP levels increase, these channels close. However, closure of K_{ATP} itself is not accountable for the shift in the potential away from the equilibrium potential of K^+, suggesting that another depolarizing component is contributing to the depolarization [14,27]. Our results suggest that TRPM4 is a key factor involved in the depolarizing current that controls the opening of VDCCs that initiates insulin secretion. Based on our results, we propose the following model: The uptake of glucose and its metabolism initiates both an increase in $[Ca^{2+}]_i$, due to release from intracellular stores [9,10] and the closure of K_{ATP} channels due to an increase in ATP. Both events may contribute to the initial membrane depolarization, since the initial rise in $[Ca^{2+}]_i$ may activate Ca^{2+}-activated cation channels and the closure of K_{ATP} channels would enhance their depolarizing effect. It remains to be determined whether the initially recruited Ca^{2+}-activated currents are carried by TRPM4 or TRPM5, which have also been found in β-cells [20], or both. In any case, the initial depolarization can reach the threshold potential of VDCCs, which further elevates $[Ca^{2+}]_i$ and induces insulin release. At this point, TRPM4 may sustain the depolarization and maintain VDCC activity to drive Ca^{2+} influx and secretion. The large increase in $[Ca^{2+}]_i$ during a depolarizing episode is followed by hyperpolarization, which may result from strong activation of Ca^{2+}-activated K^+ channels and/or re-activation of IK_{ATP} due to ATP consumption underneath the plasma membrane and/or inactivation of VDCCs. This results in a termination of the depolarization episode and causes a decrease of $[Ca^{2+}]_i$ and insulin secretion. Since β-cells exhibit many of these depolarizing episodes in an oscillatory pattern, the cell will depolarize again. This could be due to inactivation of the Ca^{2+}-activated K^+ channels, so that residual TRPM4 activity could again reach the threshold for VDCC activation. Alternatively, or in addition, oscillatory Ca^{2+} release could trigger or contribute to the next depolarizing episode in much the same way as proposed for the initial trigger event.

In this scenario, inhibition of TRPM4 function would significantly impact glucose-mediated Ca^{2+} influx and secretion as we observed with the dominant negative construct. Stimulation of insulin secretion by hormones such as AVP has also been well documented [28–30] and is thought to be involved in the amplifying pathway. In β-cells, AVP binds V_{1b} receptors coupled to Gq proteins, which signals via the PLC-β pathway leading to hydrolysis of $PtdIns(4,5)P_2$ with $Ins(1,4,5)P_3$ and DAG formation [19]. DAG activates PKC and $Ins(1,4,5)P_3$ promotes Ca2+ release from the ER. Sustained insulin secretion during hormone stimulation also requires a secondary phase due to Ca^{2+} influx [31–33]. The fact that TRPM4 suppression inhibits secretion in response to AVP stimulation suggests that it

may regulate agonist-mediated signaling in a similar way as glucose-induced mechanisms, as they both hinge on an initial Ca^{2+} release event that would lead to activation of Ca^{2+}-dependent channels such as TRPM4 and/or TRPM5. The involvement of a TRPM4-mediated depolarization in these events is further supported by the fact that secretion induced by KCl or L-arginine did not differ between controls and ΔN-TRPM4 groups, since these stimuli cause a direct cell depolarization that bypasses the requirement for TRPM4.

An important observation made during electrophysiological recordings of TRPM4 in β-cells, was that an increase in cell capacitance associated with the development of a secondary phase, where TRPM4 currents grew into several nA of magnitude. This suggests that exocytosis, a Ca^{2+}-dependent process was involved in the recruitment of additional TRPM4 channel activity. This hypothesis was confirmed by perfusion of cells with increasing $[Ca^{2+}]_i$, which resulted in a dose-dependent increase and acceleration of the secondary phase in parallel with cell capacitance. Buffered $[Ca^{2+}]_i$ at resting levels failed to induce TRPM4 translocation. These observations were made both in β-cells and HEK-293 cells. Further, loss of FM1-43 dye during elevated $[Ca^{2+}]_i$ also correlated with an increase in capacitance and the secondary phase. This led us to believe that vesicles containing TRPM4 channel were indeed recruited to the plasma membrane and this was further corroborated by confocal microscopy with fluorescent antibodies against TRPM4. Translocation of TRP channels to the plasma membrane appears to be a key event in determining their functionality. Several members of the TRP family, such as TRP-3 [34], TRPC3 [35], TRPC5 [36], TRPC6 [37] and TRPV1 [38] have been reported to translocate to the plasma membrane during exocytosis. TRPM4 translocation and activation was dependent on $[Ca^{2+}]_i$, which differs from studies with TRPC3 and TRPC6, where a Ca^{2+} independent mechanism was proposed [35,37]. Elevated $[Ca^{2+}]_i$ in the recording pipette induced concomitant TRPM4 translocation and activation, however, during receptor-mediated recruitment, an initial carbachol application increased capacitance without significant current development. This suggested translocation and incorporation of inactive channels or that the $[Ca^{2+}]_i$ levels were not high enough to reveal substantial activation of the translocated channels. The fact that these channels indeed translocated was demonstrated by a second agonist stimulation, which induced a smaller increase in $[Ca^{2+}]_i$ that was nevertheless sufficient to generate a larger current amplitude. A similar observation was reported in HEK-293 cells for heterologously expressed TRPC5 channels, where a second EGF application results in greater TRPC5 currents [36]. Secretory cells usually possess two pools of vesicles: the readily-releasable pool (RRP), which are docked with the plasma membrane and the releasable pool (RP) present in the cytoplasm awaiting for recruitment [39,40]. The kinetics of capacitance changes and translocation experiments with fluorescent TRPM4 antibodies is consistent with TRPM4 vesicles being part of the RP rather than the RRP. Recruitment of TRP channels to the plasma membrane is suggested to be involved in physiological processes such as fertilization, nociception and differentiation [35,36,38]. In the context of β-cells, it is possible that recruitment of TRPM4 may function in the support of depolarization during glucose or hormone stimulation, which typically proceed over tens of minutes.

A somewhat surprising result of this study was that the two phases of TRPM4 recruitment exhibited very similar Ca^{2+} sensitivities around ~1.2 μM in both INS-1 and HEK-293 cells (Figs. 1D and 3C). The TRPM4 sensitivity toward Ca^{2+} appears to be highly variable, with

reported EC50 values from 1 to 500 μM [5,6,41–43], possibly reflecting different experimental conditions as well as genuine regulatory mechanisms; the lowest sensitivities being observed in excised membrane patches. Factors that contribute to TRPM4's Ca^{2+} sensitivity include protein kinase C and calmodulin, which both seem to shift the apparent EC_{50} values to the left [42]. Two recent studies have proposed phosphatidylinositol 4,5-bisphosphate PIP_2 to be the most important regulator of TRPM4 [41,43], as the phospholipid greatly enhances TRPM4 Ca^{2+} sensitivity and its depletion could be the possible cause for the its desensitization. Our previous works [5,6,44] and the present study provide little indication for significant desensitization of channels in whole-cell recordings. Although the first phase of TRPM4 current, reflecting the activity of plasma membrane-resident channels, does inactivate in HEK-293 cells overexpressing TRPM4, this occurs only at Ca^{2+} levels around the EC_{50} and is not observed in INS-1 cells (Fig. 1C) or in Jurkat T-cells [6,44], which express TRPM4 natively. The secondary phase of TRPM4 current in HEK-293 cells does not inactivate and persists at plateau levels for minutes (Figs. 3 and 4). Moreover, if this inactivation were due to PIP_2 depletion, one would have expected the secondary phase to exhibit a significant right-shift in Ca^{2+} dependence, which was not observed in either HEK-293 or INS-1 cells. It should also be noted that our experimental conditions actually would favor PIP_2 breakdown, since we perfused cells with high Ca^{2+} concentrations, which might cause PLC activation and our pipette solutions were devoid of Mg-ATP, which would impede PIP_2 resynthesis. Furthermore, the vast majority of cellular PIP_2 molecules are found in the plasma membrane [45–49], suggesting that the vesicular TRPM4 channels translocating to the plasma membrane, at least initially, are not bound to PIP_2, yet respond to Ca2+ with relatively great affinity. Based on these considerations, it would seem that PIP_2 regulation of TRPM4 plays a minor role at best under our experimental conditions, which arguably are closer to physiological circumstances than excised membrane patches in which most of the PIP_2 regulation has been characterized so far.

In conclusion, this study describes a key role for TRPM4 during glucose-induced insulin secretion in β-cells. This finding may provide important insights into the etiology of some forms of type 2 diabetes, where defects in Ca^{2+} and insulin oscillations are observed. Additionally, translocation and incorporation of TRPM4 channels into the plasma membrane may represent a key short- and midterm regulatory mechanism by which β-cells regulate electrical activity. As such, the identification of TRPM4 as a key player in β-cell function also makes this channel an attractive novel candidate for drug development for diabetes.

Acknowledgments

We thank Mahealani K. Monteilh-Zoller, Carolyn E. Oki, Subhashini Srivatsan and Catherine A. Martens for technical support. We also thank Keping Qian, Y. Clare Zhang and Walter Hsu for providing their expertise and support with some of the experiments. This work was supported in part by the following grants from the National Institutes of Health: R01-AI46734 to J.-P. K., R01-GM65360 to A.F, R01-NS40927 and R01-AI50200 to R.P.

References

1. Clapham DE. TRP channels as cellular sensors. Nature. 2003; 426:517–524. [PubMed: 14654832]
2. Harteneck C, Plant TD, Schultz G. From worm to man: three subfamilies of TRP channels. Trends Neurosci. 2000; 23:159–166. [PubMed: 10717675]

3. Montell C, Birnbaumer L, Flockerzi V, Bindels RJ, Bruford EA, Caterina MJ, Clapham DE, Harteneck C, Heller S, Julius D, Kojima I, Mori Y, Penner R, Prawitt D, Scharenberg AM, Schultz G, Shimizu N, Zhu MX. A unified nomenclature for the superfamily of TRP cation channels. Mol Cell. 2002; 9:229–231. [PubMed: 11864597]
4. Xu XZ, Moebius F, Gill DL, Montell C. Regulation of melastatin, a TRP-related protein, through interaction with a cytoplasmic isoform. Proc Natl Acad Sci USA. 2001; 98:10692–10697. [PubMed: 11535825]
5. Launay P, Fleig A, Perraud AL, Scharenberg AM, Penner R, Kinet JP. TRPM4 is a Ca^{2+}-activated nonselective cation channel mediating cell membrane depolarization. Cell. 2002; 109:397–407. [PubMed: 12015988]
6. Launay P, Cheng H, Srivatsan S, Penner R, Fleig A, Kinet JP. TRPM4 regulates calcium oscillations after T cell activation. Science. 2004; 306:1374–1377. [PubMed: 15550671]
7. Earley S, Waldron BJ, Brayden JE. Critical role for transient receptor potential channel TRPM4 in myogenic constriction of cerebral arteries. Circ Res. 2004; 95:922–929. [PubMed: 15472118]
8. Guinamard R, Chatelier A, Demion M, Potreau D, Patri S, Rahmati M, Bois P. Functional characterization of a Ca^{2+}-activated non-selective cation channel in human atrial cardiomyocytes. J Physiol. 2004; 558:75–83. [PubMed: 15121803]
9. Bergsten P. Role of oscillations in membrane potential, cytoplasmic Ca^{2+}, and metabolism for plasma insulin oscillations. Diabetes. 2002; 51(Suppl 1):S171–S176. [PubMed: 11815477]
10. Gilon P, Ravier MA, Jonas JC, Henquin JC. Control mechanisms of the oscillations of insulin secretion in vitro and in vivo. Diabetes. 2002; 51(Suppl 1):S144–S151. [PubMed: 11815474]
11. Henquin JC. Triggering and amplifying pathways of regulation of insulin secretion by glucose. Diabetes. 2000; 49:1751–1760. [PubMed: 11078440]
12. Lin JM, Fabregat ME, Gomis R, Bergsten P. Pulsatile insulin release from islets isolated from three subjects with type 2 diabetes. Diabetes. 2002; 51:988–993. [PubMed: 11916916]
13. O'Rahilly S, Turner RC, Matthews DR. Impaired pulsatile secretion of insulin in relatives of patients with non-insulin-dependent diabetes. N Engl J Med. 1988; 318:1225–1230. [PubMed: 3283553]
14. Ashcroft FM, Harrison DE, Ashcroft SJ. Glucose induces closure of single potassium channels in isolated rat pancreatic beta-cells. Nature. 1984; 312:446–448. [PubMed: 6095103]
15. Barg S, Eliasson L, Renstrom E, Rorsman P. A subset of 50 secretory granules in close contact with L-type Ca^{2+} channels accounts for first-phase insulin secretion in mouse beta-cells. Diabetes. 2002; 51(Suppl 1):S74–S82. [PubMed: 11815462]
16. Berggren PO, Yang SN, Murakami M, Efanov AM, Uhles S, Kohler M, Moede T, Fernstrom A, Appelskog IB, Aspinwall CA, Zaitsev SV, Larsson O, de Vargas LM, Fecher-Trost C, Weissgerber P, Ludwig A, Leibiger B, Juntti-Berggren L, Barker CJ, Gromada J, Freichel M, Leibiger IB, Flockerzi V. Removal of Ca^{2+} channel beta3 subunit enhances Ca^{2+} oscillation frequency and insulin exocytosis. Cell. 2004; 119:273–284. [PubMed: 15479643]
17. Gopel S, Kanno T, Barg S, Galvanovskis J, Rorsman P. Voltage-gated and resting membrane currents recorded from B-cells in intact mouse pancreatic islets. J Physiol. 1999; 521(Pt 3):717–728. [PubMed: 10601501]
18. Wiser O, Trus M, Hernandez A, Renstrom E, Barg S, Rorsman P, Atlas D. The voltage sensitive Lc-type Ca^{2+} channel is functionally coupled to the exocytotic machinery. Proc Natl Acad Sci USA. 1999; 96:248–253. [PubMed: 9874804]
19. Cheng H, Yibchok-Anun S, Park SC, Hsu WH. Somatostatin-induced paradoxical increase in intracellular Ca^{2+} concentration and insulin release in the presence of arginine vasopressin in clonal HIT-T15 beta-cells. Biochem J. 2002; 364:33–39. [PubMed: 11988073]
20. Prawitt D, Monteilh-Zoller MK, Brixel L, Spangenberg C, Zabel B, Fleig A, Penner R. TRPM5 is a transient Ca^{2+}-activated cation channel responding to rapid changes in $[Ca^{2+}]_i$. Proc Natl Acad Sci USA. 2003; 100:15166–15171. [PubMed: 14634208]
21. Frodin M, Sekine N, Roche E, Filloux C, Prentki M, Wollheim CB, Van Obberghen E. Glucose, other secretagogues, and nerve growth factor stimulate mitogen-activated protein kinase in the insulin-secreting beta-cell line, INS-1. J Biol Chem. 1995; 270:7882–7889. [PubMed: 7713882]

22. Kennedy ED, Rizzuto R, Theler JM, Pralong WF, Bastianutto C, Pozzan T, Wollheim CB. Glucose-stimulated insulin secretion correlates with changes in mitochondrial and cytosolic Ca^{2+} in aequorin-expressing INS-1 cells. J Clin Invest. 1996; 98:2524–2538. [PubMed: 8958215]
23. Merglen A, Theander S, Rubi B, Chaffard G, Wollheim CB, Maechler P. Glucose sensitivity and metabolism-secretion coupling studied during two-year continuous culture in INS-IE insulinoma cells. Endocrinology. 2004; 145:667–678. [PubMed: 14592952]
24. Cochilla AJ, Angleson JK, Betz WJ. Monitoring secretory membrane with FM1-43 fluorescence. Annu Rev Neurosci. 1999; 22:1–10. [PubMed: 10202529]
25. Smith CB, Betz WJ. Simultaneous independent measurement of endocytosis and exocytosis. Nature. 1996; 380:531–534. [PubMed: 8606773]
26. Ashcroft FM, Ashcroft SJ, Harrison DE. Properties of single potassium channels modulated by glucose in rat pancreatic beta-cells. J Physiol. 1988; 400:501–527. [PubMed: 2458459]
27. Rorsman P, Eliasson L, Renstrom E, Gromada J, Barg S, Gopel S. The cell physiology of biphasic insulin secretion. News Physiol Sci. 2000; 15:72–77. [PubMed: 11390882]
28. Chen TH, Lee B, Hsu WH. Arginine vasopressin-stimulated insulin secretion and elevation of intracellular Ca^{++} concentration in rat insulinoma cells: influences of a phospholipase C inhibitor l-[6-[[17 beta-methoxyestra-1,3,5(10)-trien-17-yl]amino]hexyl]-1*H*-pyrrole-2,5-dione (U-73122) and a phospholipase A2 inhibitor *N*-(*p*-amylcinnamoyl)anthranilic acid. J Pharmacol Exp Ther. 1994; 270:900–904. [PubMed: 7932202]
29. Cheng H, Yibchok-anun S, Coy DH, Hsu WH. SSTR2 mediates the somatostatininduced increase in intracellular Ca(2+) concentration and insulin secretion in the presence of arginine vasopressin in clonal beta-cell HIT-T15. Life Sci. 2002; 71:927–936. [PubMed: 12084389]
30. Richardson SB, Laya T, VanOoy M. Similarities between hamster pancreatic islet beta (HIT) cell vasopressin receptors and V1b receptors. J Endocrinol. 1995; 147:59–65. [PubMed: 7490538]
31. Li G, Pralong WF, Pittet D, Mayr GW, Schlegel W, Wollheim CB. Inositol tetrakisphosphate isomers and elevation of cytosolic Ca^{2+} in vasopressin-stimulated insulin-secreting RINm5F cells. J Biol Chem. 1992; 267:4349–4356. [PubMed: 1311307]
32. Penner R, Neher E. The role of calcium in stimulus-secretion coupling in excitable and non-excitable cells. J Exp Biol. 1988; 139:329–345. [PubMed: 2850338]
33. Qian F, Huang P, Ma L, Kuznetsov A, Tamarina N, Philipson LH. TRP genes: candidates for nonselective cation channels and store-operated channels in insulin-secreting cells. Diabetes. 2002; 51(Suppl 1):S183–S189. [PubMed: 11815479]
34. Xu XZ, Sternberg PW. A *C. elegans* sperm TRP protein required for sperm-egg interactions during fertilization. Cell. 2003; 114:285–297. [PubMed: 12914694]
35. Singh BB, Lockwich TP, Bandyopadhyay BC, Liu X, Bollimuntha S, Brazer SC, Combs C, Das S, Leenders AG, Sheng ZH, Knepper MA, Ambudkar SV, Ambudkar IS. VAMP2-dependent exocytosis regulates plasma membrane insertion of TRPC3 channels and contributes to agonist-stimulated Ca^{2+} influx. Mol Cell. 2004; 15:635–646. [PubMed: 15327778]
36. Bezzerides VJ, Ramsey IS, Kotecha S, Greka A, Clapham DE. Rapid vesicular translocation and insertion of TRP channels. Nat Cell Biol. 2004; 6:709–720. [PubMed: 15258588]
37. Cayouette S, Lussier MP, Mathieu EL, Bousquet SM, Boulay G. Exocytotic insertion of TRPC6 channel into the plasma membrane upon Gq protein-coupled receptor activation. J Biol Chem. 2004; 279:7241–7246. [PubMed: 14662757]
38. Morenilla-Palao C, Planells-Cases R, Garcia-Sanz N, Ferrer-Montiel A. Regulated exocytosis contributes to protein kinase C potentiation of vanilloid receptor activity. J Biol Chem. 2004; 279:25665–25672. [PubMed: 15066994]
39. Duncan RR, Greaves J, Wiegand UK, Matskevich I, Bodammer G, Apps DK, Shipston MJ, Chow RH. Functional and spatial segregation of secretory vesicle pools according to vesicle age. Nature. 2003; 422:176–180. [PubMed: 12634788]
40. Pyle JL, Kavalali ET, Piedras-Renteria ES, Tsien RW. Rapid reuse of readily releasable pool vesicles at hippocampal synapses. Neuron. 2000; 28:221–231. [PubMed: 11086996]
41. Nilius B, Mahieu F, Prenen J, Janssens A, Owsianik G, Vennekens R, Voets T. The Ca^{2+}-activated cation channel TRPM4 is regulated by phosphatidylinositol 4,5-biphosphate. Embo J. 2006; 25:467–478. [PubMed: 16424899]

42. Nilius B, Prenen J, Tang J, Wang C, Owsianik G, Janssens A, Voets T, Zhu MX. Regulation of the Ca^{2+} sensitivity of the nonselective cation channel TRPM4. J Biol Chem. 2005; 280:6423–6433. [PubMed: 15590641]
43. Zhang Z, Okawa H, Wang Y, Liman ER. Phosphatidylinositol 4,5-bisphosphate rescues TRPM4 channels from desensitisation. J Biol Chem. 2005; 280:39185–39192. [PubMed: 16186107]
44. Takezawa R, Cheng H, Beck A, Ishikawa J, Launay P, Kubota H, Kinet JP, Fleig A, Yamada T, Penner R. A pyrazole derivative potently inhibits lymphocyte Ca^{2+} influx and cytokine production by facilitating transient receptor potential melastatin 4 channel activity. Mol Pharmacol. 2006; 69:1413–1420. [PubMed: 16407466]
45. Horowitz LF, Hirdes W, Suh BC, Hilgemann DW, Mackie K, Hille B. Phospholipase C in living cells: activation, inhibition, Ca^{2+} requirement, and regulation of M current. J Gen Physiol. 2005; 126:243–262. [PubMed: 16129772]
46. Micheva KD, Holz RW, Smith SJ. Regulation of presynaptic phosphatidylinositol 4,5-biphosphate by neuronal activity. J Cell Biol. 2001; 154:355–368. [PubMed: 11470824]
47. Stauffer TP, Ahn S, Meyer T. Receptor-induced transient reduction in plasma membrane PtdIns(4,5)P2 concentration monitored in living cells. Curr Biol. 1998; 8:343–346. [PubMed: 9512420]
48. Suh BC, Hille B. Regulation of ion channels by phosphatidylinositol 4,5-bisphosphate. Curr Opin Neurobiol. 2005; 15:370–378. [PubMed: 15922587]
49. Wenk MR, De Camilli P. Protein–lipid interactions and phosphoinositide metabolism in membrane traffic: insights from vesicle recycling in nerve terminals. Proc Natl Acad Sci USA. 2004; 101:8262–8269. [PubMed: 15146067]

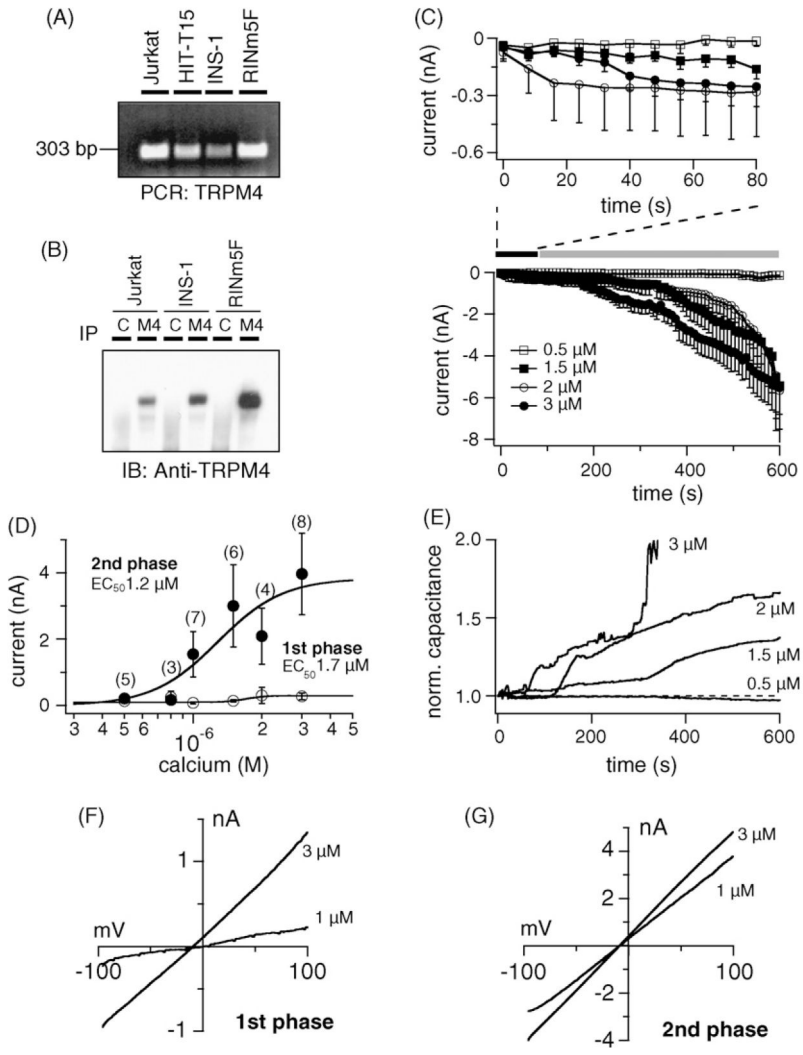

Fig. 1.

Characterization of TRPM4 currents in pancreatic β-cells. (A) Total RNA from different cell lines was isolated as described and transcribed into cDNA. RT-PCR was performed with specific primers for TRPM4. Jurkat T-lymphocytes were used as positive control. (B) Detection of TRPM4 proteins. Cells were analyzed for expression of TRPM4 protein after immunoprecipitation/immunoblotting with the polyclonal antibody against TRPM4 (M4; C indicates immunoprecipitation with an irrelevant antibody). (C) Lower panel: average inward currents carried by TRPM4 from INS-1 cells (mean ± S.E.M.) extracted at − 80 mV with $[Ca^{2+}]_i$ buffered between 0.5 and 3 µM. Upper panel: average inward currents showing the first phase during the initial 80 s after establishment of whole-cell configuration (n = 4–7 cells/concentration). Note the development of the first phase, followed by a secondary phase that is associated with increases in cell capacitance (see panel E). (D) Dose–response curves for the first and second phase of TRPM4 activation with current amplitudes extracted at +80 mV either at 80 s (first phase, open circles) or 600 s into the experiment (second phase, closed circles). (E) Normalized capacitance changes from representative cells in (C). Capacitance was normalized to the resting input capacitance measured immediately after

break-in. (F) current–voltage relationship under experimental conditions as described above, taken from a representative cell at the peak of the first phase. (G) Current–voltage relationship from representative cells taken at 600 s.

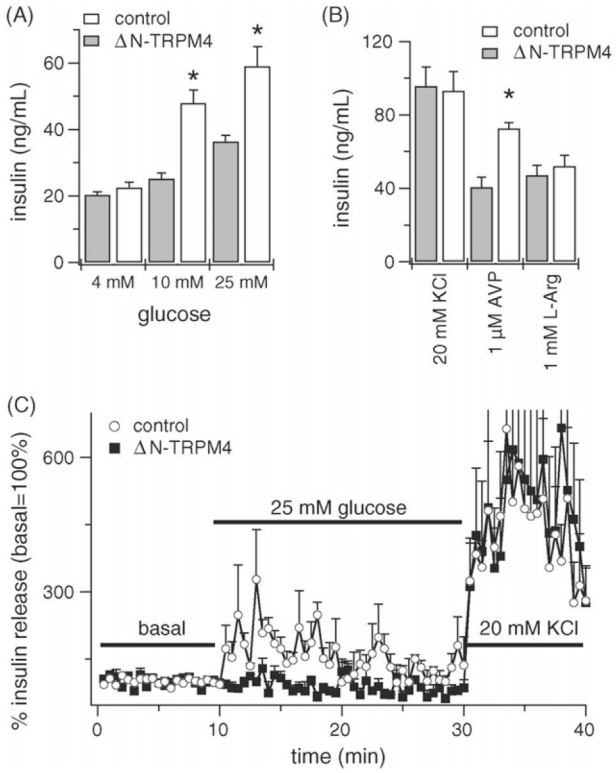

Fig. 2.

TRPM4 suppression affects insulin secretion. (A) Effect of TRPM4 protein suppression on insulin secretion under static incubation conditions. Inhibition of TRPM4 by a dominant negative effect significantly decreased the response to 10 and 25 mM glucose stimulation compared to control cells. (B) A significant decrease in insulin secretion was also observed in arginine vasopressin stimulated cells. In this experiment, the response to KCl or L-arginine did not differ. Control cells were transfected with reagents without the ΔN-TRPM4 DNA. Values are mean ± S.E.M. (n = 4 wells/treatment group from three different cell passages; $^{*}P < 0.05$ compared to same concentration). (C) Effect of TRPM4 suppression on insulin secretion under perifusion conditions. Inhibition of TRPM4 by a dominant negative effect significantly decreased the response to 25 mM glucose stimulation compared to control cells. INS-1 cells were perfused for 10 min with KRB containing 4 mM glucose to obtain a basal level and stimulated with 25 mM glucose for 20 min to induce insulin secretion. At the end, cells were depolarized with 20 mM KCl to test their viability. Control cells were transfected with reagents without the ΔN-TRPM4 DNA. Experiments represents mean ± S.E.M. (n = 3/group from three different cell passages).

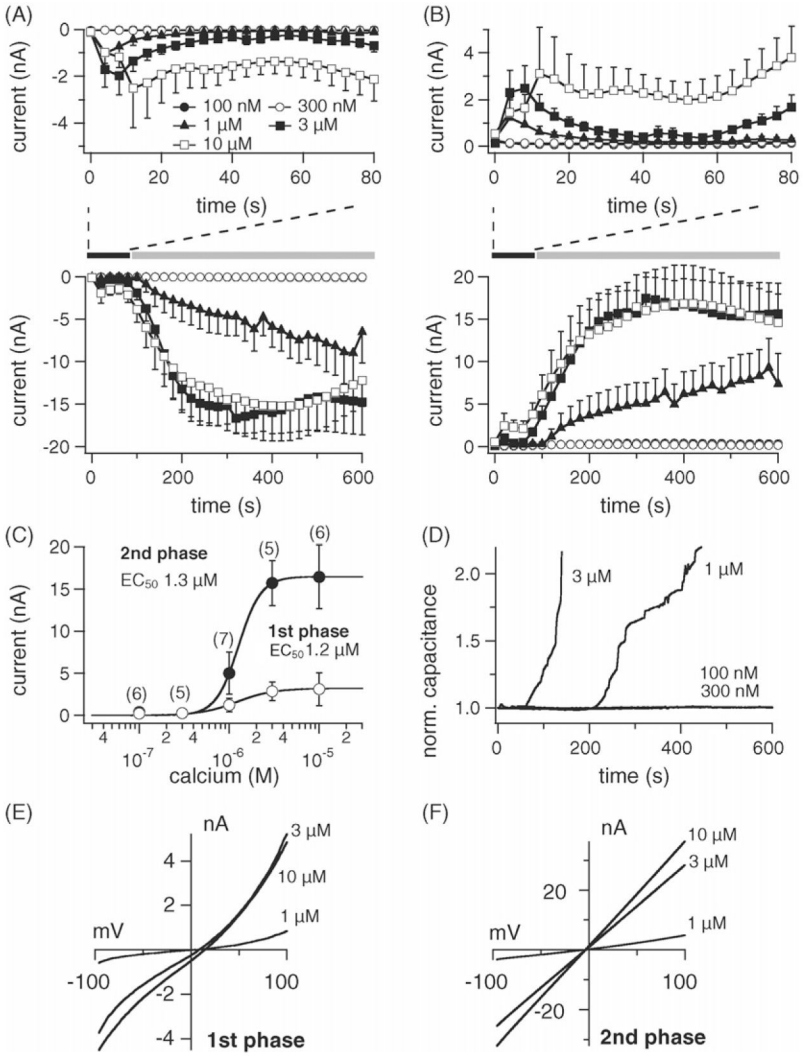

Fig. 3.

Calcium-induced exocytosis and TRPM4 activation in HEK-293 cells. (A) Lower panel: average inward currents measured in HEK-293 cells overex- pressing TRPM4 (flag-TRPM4-TrexHEK293) at −80 mV where $[Ca^{2+}]_i$ was buffered between 0.1 and 10 µM (mean ± S.E.M., n = 5–7 cells/concentration). Upper panel: average inward currents showing the first phase during the initial 80 s after establishment of whole-cell configuration. Note the development of the first phase during the initial 80 s of experiments, followed by a secondary phase that is associated with increased cell capacitance (see panel D). (B) Lower panel: average outward currents at +80 mV carried by TRPM4 from the same cells as in (A). Upper panel: average outward currents during the initial 80 s after establishment of whole-cell configuration. (C) Dose–response curves for the first and second phase of TRPM4 activation with current amplitudes extracted at +80 mV either at the peak of the first phase, or 600 s into the experiment (second phase). (D) Normalized capacitance changes from representative cells. (E) Current–voltage relationship under experimental conditions as described above, taken from representative cells at the peak of the first phase during the

initial 80 s of experiments. (F) Current–voltage relationship from the same cells as in (E) extracted at 600 s of experimental time.

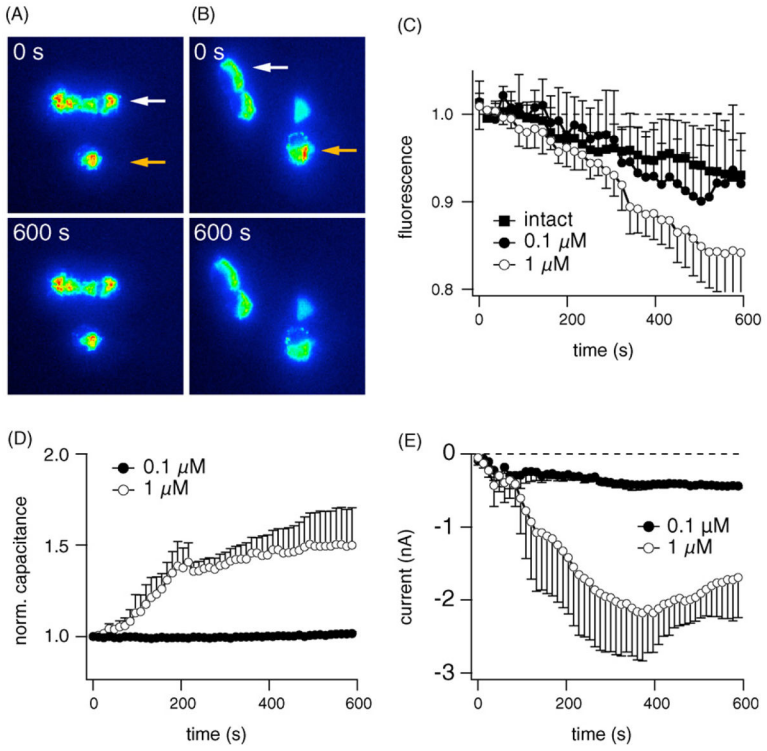

Fig. 4.

Stimulation of exocytosis results in FM1-43 dye loss and development of the secondary phase. (A) Representative fluorescence images of flag-TRPM4-TrexHEK293 cells loaded with FM1-43 and perfused with 100 nM Ca^{2+} (orange arrow) or control intact cells (white arrow) during 600 s. (B) Cells perfused with 1 μM Ca^{2+} (orange arrow) to induce exocytosis or control intact cell (white arrow) during 600 s. (C) Average fluorescence loss (mean ± S.E.M.) from cells perfused with 100 nM (n = 3) or 1 μM Ca^{2+} (n = 6) and intact controls (n = 9). (D) Average capacitance changes (mean ± S.E.M.) from cells that were patched simultaneously with fluorescence measurements (n = 3/group). (E) Average inward currents carried by TRPM4 at −80 mV from same cells in (D). (For interpretation of the references to colour in this figure legend, the reader is referred to the web version of the article.)

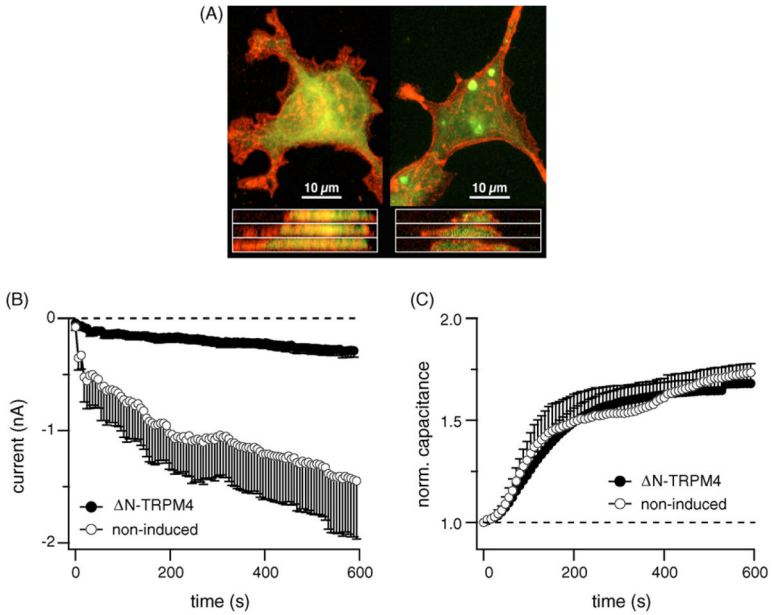

Fig. 5.

TRPM4 translocation and fusion with the plasma membrane. (A) Cellular localization of flag-TRPM4, in resting flag-TRPM4-TrexHEK293 (left panels), and l μM ionomycin treated cells (right panels), stained for flag-TRPM4 expression (red) with 2.5 mg/ml mouse anti-Flag primary antibody (Sigma), and visualized using an Alexa-568 conjugated anti-mouse secondary antibody (Invitrogen). Cell bodies were delineated using 1 mM Cell Tracker (green) prior to fixing. Confocal Z-series were taken using a BioRad 1024 inverted confocal laser microscope, with krypton/argon laser. Top panels are projected Z-stacked images taken at 0.65 mm increments through the cell, bottom panels are *z*-axis interpolated *x*-axis sections through the cell. Note the initial punctate localization of TRPM4 and shift of fluorescence to a plasma membrane localization following ionomycin treatment. (B) Average inward currents from ΔN-TRPM4 expressing cells ($n = 14$) and non-tetracycline induced control cells ($n = 7$) at −80 mV with $[Ca^{2+}]_i$ buffered at 1 μM (mean ± S.E.M.). (C) Normalized capacitance changes from ΔN-TRPM4 expressing and control cells. Inhibition of TRPM4 currents by a dominant negative effect is clearly visible, but does not alter exocytosis. (For interpretation of the references to colour in this figure legend, the reader is referred to the web version of the article.)

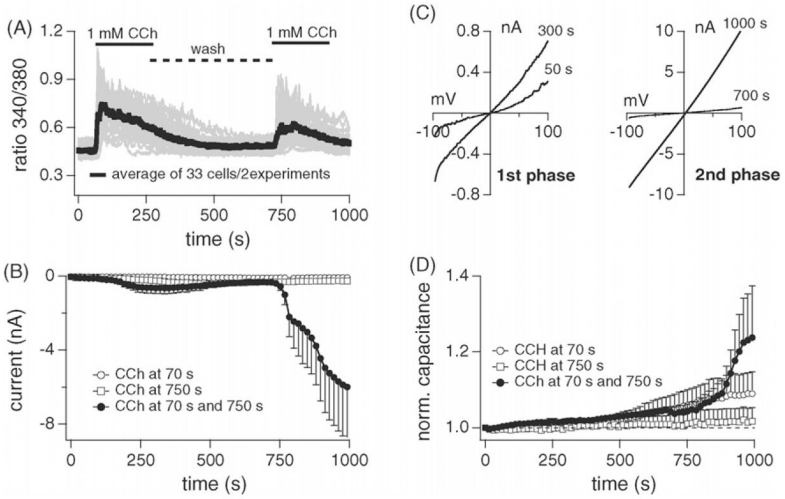

Fig. 6.

Agonist-induced secondary phase in TRPM4 current. (A) Calcium measurement from HEK293 cells overexpressing TRPM4. Cells were stimulated with carbachol twice. First, to induce exocytosis of TRPM4-containing vesicles and second to activate the new pool of TRPM4 present in the plasma membrane. (B) Average inward currents (mean ± S.E.M.) carried by TRPM4 at −80 mV under unbuffered Ca^{2+} conditions. Cells were treated with carbachol twice according to protocol used in the calcium measurement experiments ($n = 5$). Control cells were treated with carbachol at 70 s ($n = 3$) or 750 s ($n = 3$). The Ca^{2+} response to carbachol is smaller during the second application, however, the currents generated due to increased TRPM4 at the plasma membrane are much larger. (C) Current–voltage relationship typical of TRPM4 obtained from a representative cell that received double (70 and 750 s) carbachol application. (D) Average changes in capacitance from cells in (B).